

ANALYSIS OF HIGH-FIELD MAGNETIZATION PROCESS IN $\text{Sm}_2\text{Fe}_{17}\text{N}_{3.0}$

T. S. Zhao and H. M. Jin

Department of Physics, Jilin University, Changchun 130023, China

J. I. Lee and K. S. Pang

Department of Physics, Inha University, Incheon 402-751, Korea

Abstract—The observed high-field magnetization curves of $\text{Sm}_2\text{Fe}_{17}\text{N}_{3.0}$ at 4.2 K and 296 K are well reproduced by the calculation using the Sm-Fe exchange field $2\mu_B H_{\text{ex}} = 320$ K and two crystalline electric field parameters $A_0^2 = -910$ K and $A_4^0 = 200$ K. The calculation shows that during the magnetization process along the hard axis at 4.2 K, the Sm moment rotates toward the direction antiparallel to \mathbf{H} when $H < 110$ kOe and then returns to the field direction with further increase of the field. At 296 K, the Sm moment rotates toward the direction antiparallel to \mathbf{H} monotonously with increasing field and finally becomes antiparallel to \mathbf{H} when $H \geq H_A = 210$ kOe. The particular magnetization process of the Sm moment can be explained by the field-induced noncollinear coupling between the spin and orbital moments of the Sm ion.

I. INTRODUCTION

In recent years, the intrinsic magnetic properties of R_2Fe_{17} compounds have been improved considerably by introducing interstitial nitrogen atoms to form $\text{R}_2\text{Fe}_{17}\text{N}_x$ compounds. [1] The nitride $\text{Sm}_2\text{Fe}_{17}\text{N}_x$ exhibits strong uniaxial anisotropy at room temperature with $H_A = 140 \sim 210$ kOe, [2-4] which makes $\text{Sm}_2\text{Fe}_{17}\text{N}_x$ a very promising material for permanent magnet applications. The High-field magnetization curves at 4.2 K and 296 K were measured on the magnetically aligned powder $\text{Sm}_2\text{Fe}_{17}\text{N}_{3.0}$ samples by Kato et al.. [5] In this paper, we shall report the analysis of the magnetization process of the Fe and Sm sublattices in $\text{Sm}_2\text{Fe}_{17}\text{N}_{3.0}$ in terms of the exchange and crystalline electric field (CEF) model. It will be shown that the field-induced noncollinear coupling between the spin and orbital moments of the Sm ion causes a particular magnetization process of the Sm moment when the field is applied along the hard axis.

II. METHOD OF CALCULATION

$\text{Sm}_2\text{Fe}_{17}\text{N}_{3.0}$ crystallizes in the rhombohedral $\text{Th}_2\text{-Zn}_{17}$ -type structure, in which the Sm ions occupy the single 6c site. In the presence of an external magnetic field \mathbf{H} , the Hamiltonian describing the 4f electrons of the Sm ion in $\text{Sm}_2\text{Fe}_{17}\text{N}_{3.0}$ is given by

$$\mathcal{H} = \lambda \mathbf{L} \cdot \mathbf{S} + \mathcal{H}_{\text{CEF}} + 2\mu_B \mathbf{S} \cdot \mathbf{H}_{\text{ex}} + \mu_B (\mathbf{L} + 2\mathbf{S}) \cdot \mathbf{H}, \quad (1)$$

where λ is the spin-orbit coupling constant, \mathbf{L} and \mathbf{S} are the total orbital and spin angular momenta, \mathcal{H}_{CEF} is the CEF Hamiltonian, and \mathbf{H}_{ex} is the Sm-Fe exchange field.

Since the sixth-order Stevens coefficient γ_J is zero for the ground-state $J = \frac{5}{2}$ multiplet of the Sm ion, the diagonal A_6^0 term in the CEF Hamiltonian, through mixing

of the excited multiplets, has a smaller influence on the uniaxial anisotropy than the A_4^0 term. Neglecting the off-diagonal and sixth-order CEF terms, the CEF Hamiltonian of the Sm ion can be simply written as

$$\mathcal{H}_{\text{CEF}} = A_2^0 \sum_j \sqrt{\frac{4\pi}{5}} Y_2^0(\theta_j, \varphi_j) + A_4^0 \sum_j \sqrt{\frac{4\pi}{9}} Y_4^0(\theta_j, \varphi_j), \quad (2)$$

where A_n^0 ($n = 2, 4$) are the CEF parameters in which the 4f radial expectation values $\langle r^n \rangle$ are involved, and the summation j is over all the 4f electrons.

The matrix elements of Eq. (1) are calculated by using the irreducible tensor operator technique. [6] Two first excited multiplets ($J = \frac{7}{2}$ and $J = \frac{9}{2}$) are taken into account in the calculation. For the spin-orbit coupling $\lambda = 410$ K is used, corresponding to an energy separation of 1435 K between $J = \frac{5}{2}$ and $J = \frac{7}{2}$ multiplets of the trivalent Sm free ion. [7] The eigenvalues E_n and eigenfunctions $|n\rangle$ ($n = 1, 2, \dots, \sum_J (2J+1) = 24$) are obtained by diagonalizing the 24×24 matrix of Eq. (1). The free energy for the $\text{Sm}_2\text{Fe}_{17}\text{N}_{3.0}$ system is given by

$$F(T, \mathbf{H}, \mathbf{H}_{\text{ex}}) = -2k_B T \ln Z + K_1 \sin^2 \theta_{\text{Fe}} - \mathbf{M}_{\text{Fe}} \cdot \mathbf{H}, \quad (3)$$

$$Z = \sum_n \exp(-E_n/k_B T), \quad (4)$$

where K_1 and M_{Fe} are the magnetic anisotropy constant and the magnetic moment of the Fe sublattice per formula unit, respectively. $\mathbf{H}_{\text{ex}}(T)$ is assumed to be proportional and antiparallel to $\mathbf{M}_{\text{Fe}}(T)$. For given temperature T and magnetic field \mathbf{H} , the equilibrium direction of \mathbf{M}_{Fe} can be determined by minimizing the free energy $F(T, \mathbf{H}, \mathbf{H}_{\text{ex}})$ with respect to the angle θ_{Fe} . The magnetic moment of the Sm ion is given by

$$\mathbf{M}_{\text{Sm}} = \mathbf{M}_{\text{Sm}}^{\text{L}} + \mathbf{M}_{\text{Sm}}^{\text{S}}, \quad (5)$$

where $\mathbf{M}_{\text{Sm}}^{\text{L}}$ and $\mathbf{M}_{\text{Sm}}^{\text{S}}$ represent the orbital and spin moments of the Sm ion, respectively, and can be calculated

as

$$M_{Sm}^L = - \sum_n \mu_B \langle n | L | n \rangle \frac{\exp(-E_n/k_B T)}{Z}, \quad (6)$$

$$M_{Sm}^S = - \sum_n \mu_B \langle n | 2S | n \rangle \frac{\exp(-E_n/k_B T)}{Z}. \quad (7)$$

The total magnetic moment of the system can be obtained by

$$M = 2M_{Sm} + M_{Fe}. \quad (8)$$

In the calculation, the reduced temperature dependence of $K_1(T/T_c)/K_1(0)$ and $M_{Fe}(T/T_c)/M_{Fe}(0)$ for $Sm_2Fe_{17}N_{3.0}$ is assumed to be identical with those for Y_2Fe_{17} . [8] From the magnetization curves of $Y_2Fe_{17}N_x$ measured parallel and perpendicular to the alignment direction at 4.2 K, the anisotropy field was estimated to be about 40 kOe, which corresponds to $K_1(0) = -53$ K/f.u.. [9] The value for $M_{Fe}(0)$ is taken to be $39.2\mu_B/f.u.$

III. RESULT AND DISCUSSION

Figure 1 shows the calculated and experimental magnetization curves at 4.2 K and 296 K for $Sm_2Fe_{17}N_{3.0}$. The dashed lines in Fig. 1 represent the calculation that

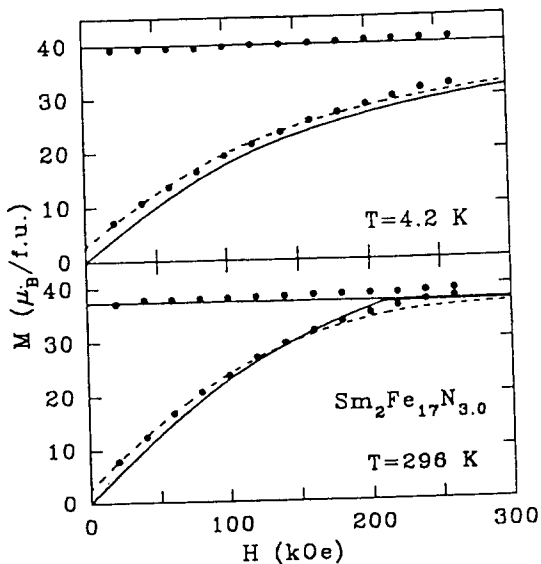


FIG. 1. The calculated and experimental magnetization curves at 4.2 K and 296 K for $Sm_2Fe_{17}N_{3.0}$. the solid and dashed lines represent the calculation with the applied field parallel and perpendicular to the c axis and making an angle of 86° with the c axis, respectively. Experimental data (full circles) are taken from Ref. 5.

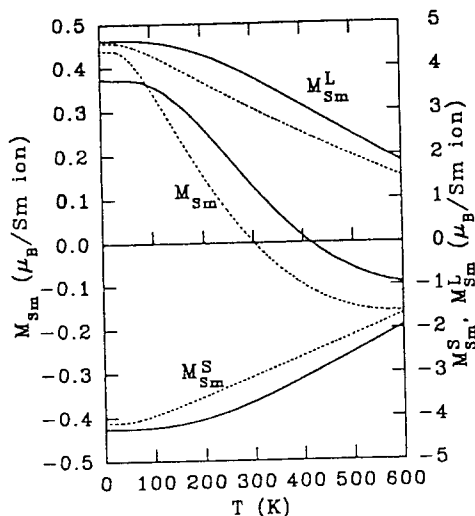


FIG. 2. The calculated M_{Sm} , M_{Sm}^L and M_{Sm}^S as a function of temperature. The dashed lines represent the calculation not including the CEF interaction.

the external field H makes an angle of 86° with the c -axis, which simulates a situation of incomplete c -axis alignment of powder particles. Following set of parameters: $A_2^0 = -910$ K, $A_4^0 = 200$ K, and $2\mu_B H_{ex}(0) = 320$ K are

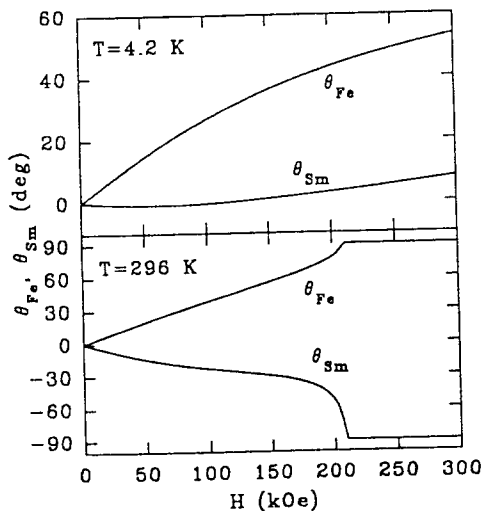


FIG. 3. The calculated field dependence of the angles θ_{Fe} and θ_{Sm} when the field is applied perpendicular to the c axis at 4.2 K and 296 K.

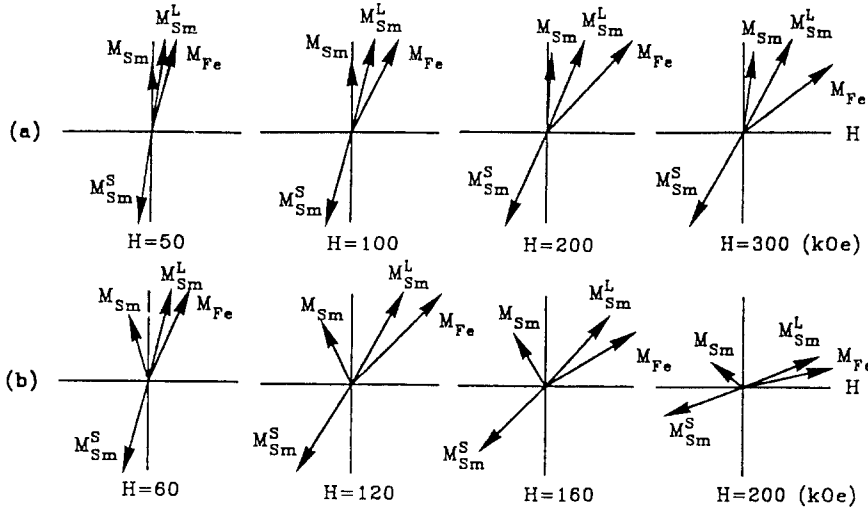


FIG. 4. The magnetic structures of $\text{Sm}_2\text{Fe}_{17}\text{N}_{3.0}$ at different field strengths at (a) $T=4.2$ K and (b) 296 K.

used in the calculation. It can be seen from Fig.1 that the present calculation reproduce well the experiment. The value of the anisotropy field H_A at 296 K is calculated to be 210 kOe for $\text{Sm}_2\text{Fe}_{17}\text{N}_{3.0}$, which may be compared with $H_A = 214$ kOe for $\text{Sm}_2\text{Fe}_{17}\text{N}_{2.94}$ determined by the singular point detection technique. [2] The anisotropy field H_A at 4.2 K is estimated to be more than 1300 kOe by the calculation.

The temperature dependence of the Sm magnetic moment and the magnetization process of the Sm and Fe sublattices in $\text{Sm}_2\text{Fe}_{17}\text{N}_{3.0}$ are analyzed by the calculation using the determined CEF and Sm-Fe exchange field parameters. Figure 2 shows the calculated temperature dependence of M_{Sm} , M_{Sm}^L , and M_{Sm}^S at zero magnetic field. The calculated values of M_{Sm} are $0.372\mu_B$ and $0.136\mu_B$ at 4.2 K and 296 K, respectively. The crossover temperature T_∞ , at which the total Sm moment because negative, is found to be 418 K. The dashed lines in Fig. 2 represent the calculation that did not take the CEF interaction into account. In this case, the value of T_∞ is reduced to 301 K, indicating that the CEF interaction has a striking influence on the crossover temperature.

Figure 3 shows the calculated magnetic field dependence of the angles θ_{Fe} and θ_{Sm} for $\text{Sm}_2\text{Fe}_{17}\text{N}_{3.0}$ when the

field is applied perpendicular to the c axis at 4.2 and 296 K. At 4.2 K, \mathbf{M}_{Fe} rotates toward the \mathbf{H} direction continuously, while \mathbf{M}_{Sm} rotates toward the direction antiparallel to \mathbf{H} with small θ_{Sm} value when $H < 110$ kOe and then returns to the field direction with further increase of the field. There exists a very pronounced noncollinearity between \mathbf{M}_{Fe} and \mathbf{M}_{Sm} . The angle between \mathbf{M}_{Fe} and \mathbf{M}_{Sm} amount to as high as $\Delta\theta = \theta_{\text{Fe}} - \theta_{\text{Sm}} = 45.7^\circ$ at 300 kOe. At 296 K, \mathbf{M}_{Sm} rotates toward the direction antiparallel to \mathbf{H} monotonously with increasing field and, finally, becomes antiparallel to \mathbf{H} when $H \geq H_A = 210$ kOe. The particular magnetization process of \mathbf{M}_{Sm} mentioned above is caused by the field-induced noncollinear coupling between \mathbf{M}_{Sm}^L and \mathbf{M}_{Sm}^S . Because of the weak spin-orbit coupling of the Sm ion, a noncollinear coupling between \mathbf{M}_{Sm}^L and \mathbf{M}_{Sm}^S will occur under the strongly combined action of the CEF, the Sm-Fe exchange field and the external field. The maximum angle between \mathbf{M}_{Sm}^L and $-\mathbf{M}_{\text{Sm}}^S$ reaches more than 2° . Figures 4(a) and 4(b) illustrate the variation of the magnetic structures of $\text{Sm}_2\text{Fe}_{17}\text{N}_{3.0}$ at 4.2 K and 296 K. At 4.2 K, due to the fact that M_{Sm}^L is always larger than M_{Sm}^S ($M_{\text{Sm}}^L - M_{\text{Sm}}^S \sim 0.4\mu_B$), the total Sm moment \mathbf{M}_{Sm} is closer to \mathbf{M}_{Sm}^L than \mathbf{M}_{Sm}^S , and is located in the region

marked by the c axis and \mathbf{H} when $H > 110$ kOe [see Fig. 4(a)]. At 296 K, however, the value difference between M_{Sm}^L and M_{Sm}^S is small ($|M_{\text{Sm}}^L - M_{\text{Sm}}^S| < 0.14\mu_B$), resulting in a fact that \mathbf{M}_{Sm} is located in the region marked by the c axis and $-\mathbf{H}$ [see Fig. 4(b)]. In addition, the values of M_{Sm}^L and M_{Sm}^S decrease with increasing field. For instance, M_{Sm}^L and M_{Sm}^S vary from $3.625\mu_B$ and $3.512\mu_B$ at 80 kOe to $3.114\mu_B$ and $3.083\mu_B$ at 160 kOe. When H exceeds 178 kOe, M_{Sm}^S becomes larger than M_{Sm}^L , and \mathbf{M}_{Sm} finally becomes antiparallel to \mathbf{H} when $H \geq H_A$.

ACKNOWLEDGMENTS

This work was supported by the National Natural Science Foundation of China. This work was also supported by the 1995 Inha University Research Fund and by the Basic Science Research Institute Program, Ministry of Education, 1995 (BSRI-95-2430).

REFERENCES

- [1] K.H.J. Buschow, Rep. Prog. Phys. **54**, 1123 (1991).
- [2] M. Katter, J. Wecker, C. Kuhrt, L. Schuit, and R. Grössinger, J. Magn. Magn. Mater. **114**, 35 (1992).
- [3] T. Iriyama, K. Kobayashi, N. Imaoka, T. Fukuda, H. Kato, and Y. Nakagawa, IEEE Trans. Magn. **28**, 2326 (1992).
- [4] M. Katter, J. Wecker, D. Kuhrt, L. Schuit, and R. Grössinger, J. Magn. Magn. Mater. **117**, 419 (1992).
- [5] H. Kato, M. Yamada, G. Kido, Y. Nakagawa, T. Iriyama, and K. Kobayashi, J. Appl. Phys. **73**, 6931 (1993).
- [6] B.G. Wybourne, *Spectroscopic Properties of Rare Earth*, Wiley-Interscience, New York, 1965.
- [7] S. Hufner, *Optical Spectra of Transparent Rare-Earth Compounds*, Academic, London, 1978, p.34.
- [8] R. Verhoef, Thesis, University of Amsterdam, 1990.
- [9] J.P. Liu, K. Bakker, F.R. de Boer, T.H. Jacobs, and K.H.J. Buschow, J. Less-Common Met. **170**, 109 (1991).